Published in final edited form as:
Neurobiol Dis. 2011 December ; 44(3): 270–276. doi:10.1016/j.nbd.2011.06.019.

Deficiency in the inner mitochondrial membrane peptidase 2-like (Immp21) gene increases ischemic brain damage and impairs mitochondrial function

Yi Ma[a,b], **Suresh L. Mehta**[a], **Baisong Lu**[c], and **P. Andy Li**[a,*]

[a]Department of Pharmaceutical Sciences, Biomanufacturing Research Institute and Technology Enterprise (BRITE), North Carolina Central University, Durham, NC USA

[b]Department of Pathology, Ningxia Medical University, Yinchuan, Ningxia, P. R. China

[c]Institute for Regenerative Medicine, Wake Forest University School of Medicine, Winston-Salem, NC USA

Abstract

Mitochondrial dysfunction plays an important role in mediating ischemic brain damage. Immp2l is an inner mitochondrial membrane peptidase that processes mitochondrial proteins cytochrome *c*1 (Cyc1). Homozygous mutation of Immp2l (Immp2l$^{Tg(Tyr)979Ove}$ or Immp2l$^{-/-}$) elevates mitochondrial membrane potential, increases superoxide ($\bullet O_2^-$) production in the brain and impairs fertility. The objectives of this study are to explore the effects of heterozygous mutation of lmmp2l (Immp2l$^{+/-}$) on ischemic outcome and to determine the influence of Immp2l deficiency on brain mitochondria after stroke. Male Immp2l$^{+/-}$ and wild-type (WT) mice were subjected to 1-h focal cerebral ischemia. Their brains were harvested after 5 and 24-h of reperfusion. The results showed that infarct volume and DNA oxidative damage significantly increased in the Immp2l$^{+/-}$ mice. There were no obvious cerebral vasculature abnormalities between the two types of mice viewed by Indian ink perfusion. The increased damage in Immp2l$^{+/-}$ mice was associated with early increase in $\bullet O_2^-$ production. Mitochondrial respiratory rate, total mitochondrial respiratory capacity and mitochondrial respiratory complex activities were decreased at 5-h of recirculation in Immp2l$^{+/-}$ mice compared to WT mice. Our results suggest that lmmp2l deficiency increases ischemic brain damage by enhancing $\bullet O_2^-$ production and damaging mitochondrial functional performance.

Keywords

Cerebral ischemia; Cell death mechanisms; Focal ischemia; Gene regulation; Immp2l; Immunohistochemistry; Mitochondria; Reperfusion

*Correspondence: Dr. PA Li, BRITE Institute, North Carolina Central University, 1801 Fayetteville Street, Durham, NC 27707, USA. pli@nccu.edu, Tel: 1-919-530 6872, Fax: 1-919-530-6600.

Statement of conflict of interests: The authors declare that they have no potential conflict of interest.

Introduction

Mitochondrial inner membrane peptidase (Imp) is a signal peptidase complex responsible for proteolytic processing of certain precursor or intermediate polypeptides that are exported from matrix. In yeast, the peptidase is comprised by two catalytic (Imp1 and Imp2) and one non-catalytic (Som1) subunits. Homologues of Imp in the mammalian genome are Imp1 inner mitochondrial membrane peptidase-like (Immp1l) and Imp2 inner mitochondrial membrane peptidase-like (Immp2l). The substrate for Imp2 is Cyc1 and mitochondrial glycerol phosphate dehydrogenase 2 (GPD2) and those for Imp1 include GPD2, cytochrome *b2*, cytochrome *c* oxidase subunit II, and NADH-cytochrome *b5* reductase (Behrens et al., 1991; Nunnari et al., 1993; Esser et al., 2004). While deletion of Imp1 in yeast is lethal, deletion of Imp2 affects the processing of Cyc1 signal peptide. Cyc1 need to be processed through two steps in order to exert proper function in mitochondrial electron transport. Incomplete processing of Cyc1 may hamper electron transport. Functions of Immp1l remain unknown at this time. Mutation of Immp2l gene has been linked to Gilles de la Tourette syndrome, a neurological disorder characterized by multiple involuntary motor and vocal tics (Petek et al., 2001). In two recent studies, it was observed that homozygous mutation of human lmmp2l gene in mouse results in impaired gametogenesis and erectile dysfunction in males, infertility in females, and bladder dysfunction in both (Lu et al., 2008; Soler et al., 2010). These manifestations are likely associated with impairment of signal peptide sequence processing of Cyc1, hyperpolarization of mitochondrial membrane potential, increased production of $\bullet O_2^-$, and insufficient availability of nitric oxide (Lu et al., 2008).

Mitochondrial plays a central role in pathophysiology of many neurodegenerative diseases, including stroke. Increased free radical production from mitochondria triggers formation of a mitochondrial permeability transition pore (mPTP), which leads to release of pro-apoptotic proteins such as cytochorome c and apoptosis-inducing factor (AIF). The consequence is activation of cell death pathways and eventually cell death (Chen *et al*, 1998; Crompton *et al*, 2002; Di Lisa *et al*, 2003; Halestrap 2006; Yu *et al*, 2009; Martin *et al*, 2010). Studying the mitochondrial proteins under normal and pathological conditions will assist us to acquire critical knowledge toward our understanding to mitochondria and mitochondria-associated diseases. Since deletion Immp2l causes incomplete cleavage of Cyc1 that leads to increased ROS and the brain is a lipid-rich organ that is extremely sensitive to ROS, we hypothesize that deficiency in lmmp2l gene may exacerbate mitochondrial dysfunction and increase brain damage after middle cerebral artery occlusion (MCAO). To test this hypothesis, we induced 1-h of MCAO in WT and Immp2l$^{+/-}$ mice and collected their brains at 5- and 24-h of recirculation. Our results demonstrated that deficiency in Immp2l gene increased cerebral infarct volume and oxidative DNA damage after MCAO. The enhanced brain damage in Immp2l$^{+/-}$ mice was associated with elevation of ROS production and suppression of mitochondrial respiration control ratio (RCR) and electron transport chain complexes II+III, and IV activities in early reperfusion stage after transient focal ischemia.

Materials and Methods

Experimental Animals

Seventy-five male mice, 39 WT Friend Virus B NIH Jackson (FVB/N) and 36 Immp2l$^{+/-}$ mice, weighing 18 to 20 g, were used in this study. All animal procedures were performed in accordance with the NIH Guide for Care and Use of Laboratory Animals and were approved by the Institutional Animal Care and Use Committee at North Carolina Central University. Breeding pairs of Immp2l$^{+/-}$ mice were obtained from Dr. Lu's laboratory at Wake Forest University School of Medicine and their off-springs were genotyped. Heterozygous Immp2l mutant mice were used in the present studies based on the consideration that homozygous Immp2l mutation mice have been shown to exhibit increased ROS production and

mitochondrial dysfunction at basal level (Lu et al 2008) and to accelerate aging (George et al 2011). It is therefore predictable that the Immp2l$^{-/-}$ animals are going to be vulnerable to ischemic injury. Studying the Immp2l+/− mice, who showed no altered ROS levels under physiological condition, challenged by ischemia and reperfusion injury may help to better understand the importance of this mitochondrial peptidase in health and disease conditions.

The Immp2l$^{+/-}$ mice have been maintained for at least 18 months by the time of the current manuscript submission. These mice gain the same weight as the wildtype and no other gross abnormality. The only phenotypical character that has been observed in this colony is change in hair color to light grey or dusty white. The lmmp2l$^{+/-}$ and WT littermates were used in this study. Animals were divided into sham-operated controls, ischemia plus 5- and 24-h of reperfusion. Numbers of animals used in the various experimental groups are given in figure legends.

Mouse model of focal cerebral ischemia

Prior to the induction of ischemia, mice were fasted overnight with free access to water. Animal fasting blood glucose levels were between 4 and 6 mM. Anesthesia was induced by inhalation of 3.5% isoflurane in a mixture of N_2O:O_2 (70:30) and maintained at 1–1.5% isoflurane with a facial mask during surgical procedures. Body temperature was maintained to 37±0.5°C by a combination of a heating lamp and a heating blanket (T/Pump, TP650, Gaymar Industries, Inc, Orchard Park, NY, USA). Transient MCAO was induced by the intraluminal filament technique as previously described (Koizumi et al., 1986; Haines et al., 2010). For reperfusion, mice were re-anesthetized and the filament was removed after 1-h of MCAO to restore blood flow. After MCAO, neurologic behaviors were examined, and only animals with neurological signs of diminished resistance to lateral push, walking to the left after being pulled backwards by the tail, or with spontaneous contralateral circling were included in the study. Five mice were excluded due to surgical failure. Upon predetermined end points (5- and 24-h of reperfusion), animals were either perfusion-fixed with 4% paraformaldehyde or euthanized. Brain samples used for immunohistochemistry were sectioned on a vibrating microtome (VT1000S, Leica Microsystems, Wetzlar, Germany) and those for mitochondrial function measurements were processed immediately for mitochondria isolation.

Measurement of infarct volume

At 24-h of reperfusion, animals (10 WT and 7 Immp2l$^{+/-}$) were deeply anesthetized with 5% isoflurane and transcardially perfused with ice-cold PBS. Brains were sectioned in mouse brain matrix (Harvard Apparatus, Holliston, MA, USA) at a thickness of 1 mm. Seven coronal sections were obtained between Bregma 3.7 mm and −6.04 mm and incubated with 2% of 2,3,5-triphenyltetrazolium chloride (TTC) for 15 minutes at room temperature. Brain slices were then fixed in 4% paraformaldehyde and electronically scanned for acquisition and image processing. Infarct areas on each brain sections were measured using NIH Image J software (rsb.info.nih.gov/nih-image) and infarct volumes were calculated from all sections with corrections of intersection distance.

Anatomy of the MCA and Circle of Willis

Naïve mice (n=3 in each type of mouse) were deeply anesthetized and transcardially perfused with 0.1M phosphate buffer (pH 7.4) to flush out the blood. Mouse was then injected with Indian ink (25%) made in 6% gelatin and 0.1M Phosphate buffer. Temperature during perfusion was maintained at 37°C. After perfusion brain was cooled to allow gelatin solidification and fixed with 4% paraformaldehyde. Brain images were captured using a Nikon digital camera.

In situ detection of $\bullet O_2^-$ production

Animals were injected with 200 μl (1 mg/kg) of dihydroethidine (DHE, Molecular Probes In. Eugene, OR, USA) intravenously 20–30 minutes before MCAO through a tail vein to view superoxide formation (Zhao et al., 2003). Brains were briefly perfusion-fixed with 4% paraformaldehyde at 5-h of reperfusion. The brains were removed and sectioned coronally at 30 μm thickness in ice-cold phosphate-buffered saline bath with a vibrating microtome (VT1000S). Four coronal brain sections from Bregma 1.70 to −4.20 mm were selected and mounted with Vectashield mounting medium (Vector Laboratories, Burlingame, CA, USA) containing DAPI to view nuclear morphology. Three pre-selected microscopic fields at 400X magnification from the cortical and striatal regions of ipsilateral hemisphere of each mouse were captured with a Nikon confocal laser-scanning microscope (ECLIPSE Ti-U, Nikon Instruments Inc. Melville, NY). Fluorescence intensity of the oxidized DHE was measured using NIS Elements software (Nikon Instruments Inc. Melville, NY, USA).

Oxidative DNA Damage

At 5- and 24-h of reperfusion, animals (n=4 per group) were perfusion-fixed with 4% paraformaldehyde. The brains were post-fixed in the same solution, and sectioned at 30 μm thicknesses using a vibrating microtome (VT1000S, Leica). After being washed with Tris-buffered saline containing 0.1% triton X-100 and blocked with 3% BSA, the sections were incubated overnight with primary mouse monoclonal antibody (1:1000 dilution, clone 15A3, Abcam Cambridge, MA, USA) for 8-hydroxy-2-deoxyguanosine (8-OHdG), a marker for DNA oxidative damage. The sections were then incubated with Alexa Fluor 488 conjugated secondary antibody (1:500; InVitrogen, Eugene, Oregon, USA) for 2-h at room temperature. The sections were mounted on glass slides using Vectashield mounting medium (Vector Laboratories, Burlingame, CA, USA) containing propidium iodide. Three pre-selected anatomical spots in the ipsilateral striatum and cortex were selected for image capture. Images were captured using a Nikon laser-scanning confocal microscope (ECLIPSE Ti-U, Nikon Instruments) at a 400X magnification. The number of 8-OHdG-positive stained cells were counted using NIH Image J software (rsb.info.nih.gov/nih-image).

Measurements of mitochondrial respiration and complex activities

The cerebral cortical and striatal areas of the control and ischemic mice with 5-h recovery were rapidly dissected and homogenized in 10 volumes of the 1x Extraction Buffer (MITOSIO1, Sigma) containing isotonic solution of mM HEPES, pH 7.5, 200 mM mannitol, 70 mM sucrose, 1 mM EGTA and 2 mg/ml dilapidated BSA. The homogenate was centrifuged at 600*g* for 5 min, the supernatant was removed, and the pellet was resuspended with 1x Extraction Buffer. The resuspended pellet was centrifuged again at 11,000*g* for 10 min. The final pellet was resuspended in 1x Extraction Buffer (~40 ml/100 mg tissue). Protein concentrations were determined with a Bio-Rad protein assay (Bio-Rad) and 0.2 mg of protein was used for respiration studies. Mitochondrial respirations at different complexes were assessed in a peltier temperature-controlled two chamber high-resolution respirometer (O2K, Oroboros Instruments, Austria) at 37°C. To avoid any potential oxygen limitation, all experiments were conducted after hyperoxygenation (approximately 400 nmol O_2/ml). Briefly, isolated mitochondria were incubated in mitochondrial respiration medium MiR05 (110 mM sucrose, 0.5 mM EGTA, 3.0 mM $MgCl_2$, 80 mM KCl, 60 mM K-lactobionate, 10 mM KH_2PO_4, 20 mM Taurine, 20 mM HEPES, 1.0 g/l BSA, pH 7.1) and respiration was initiated using saturating amounts of ADP (5 mM) following the addition of glutamate (10 mM) and malate (5 mM) for complex I, succinate (10 mM) and rotenone (0.5 μM) for complex II+III, and TMPD/ascorbate (0.5/2 mM) and antimycin A (2.5 μM) for complex IV. RCR was calculated as the ratio of respiration induced in the presence of ADP (state 3 respiration) to the respiration when ADP is completely utilized (state 4 respiration). Oligomycin was added to eliminate the

contribution of ATP cycling hydrolysis by contaminating ATPases and resynthesis by the mitochondrial ATP synthase to state 4 respiration. Total mitochondrial respiratory capacity (MRC) of isolated mitochondria in WT and Immp2l$^{+/-}$ mice was subsequently measured by titration with 5 nM carbonyl cyanide p-(trifluoromethoxy) phenylhydrazone (FCCP).

Statistics

All data are presented as means ± s.d. Student's t-test was used to analyze the difference in infarct volume between the two animal species. One-way ANOVA followed by Tukey's test was used to analyze the data for $\bullet O_2^-$, DNA oxidative damage, and mitochondrial functions. A p value <0.05 was considered as significant.

Results

Enlargement of Infarct Volume

Focal ischemia of 1-h duration induced brain infarct in the striatum, slightly reaching to overlaying cortex, in WT mice at 24-h of reperfusion. The infarct volume was significantly enlarged in lmmp2l$^{+/-}$ mice compared with the WT mice, covering both the striatum and the cortex (Fig. 1A). As a result, the infarct volume increased from 12.1±9.0 percent hemisphere in the WT mice to 30.9±14.1 percent in Immp2l$^{+/-}$ mice (Fig. 1B). Brain edema was also calculated by comparing the volume of ipsilateral to that of contralateral hemisphere. There is no significant difference between the two groups albeit there is trend that Immp2l$^{+/-}$ mice tend to have bigger increase in edema.

Cerebral Vasculature

To evaluate whether Immp2l deficiency causes phenotypic changes in the cerebral vasculature, we transcardially injected Indian black ink and imaged the cerebral blood vessels (Fig. 2). Both WT and Immp2l^{+}/$^{-}$ mice showed intact and correct alignment of the Circle of Willis, anterior, middle, and posterior cerebral arteries with no remarkable difference.

Enhanced $\bullet O_2^-$ Production

Superoxide production was detected *in situ* using DHE fluorescent probe. DHE specifically reacts with intracellular $\bullet O_2^-$ and forms precipitates that emit red fluorescence under excitation and emission wave length of 480 nm and 567 nm, respectively (Zhao *et al*, 2003). Quantification of red fluorescence intensity revealed that a small amount of $\bullet O_2^-$ was produced in animals at the baseline without being subjected to ischemia. Ischemia of 1-h duration resulted in a significant production of $\bullet O_2^-$ at 5-h of recovery in the ischemic cortex and striatum of the WT mice compared to non-ischemic control animals (p<0.001). Superoxide production in lmmp2l$^{+/-}$ mice further increased at 5-h of recirculation in the cortex and striatum when compared to control animals, as well as to WT mice at 5-h of reperfusion. Fig. 3A and 3B are microphotogram showing DHE staining obtained from the cortex and striatum of the WT and Immp2l$^{+/-}$ mice, respectively. Summarized data are given in Fig. 3C and 3D.

DNA damage

DNA oxidation results, as determined by anti-8-OHdG antibody staining on sections obtained from WT and Immp2l$^{+/-}$ mice, showed no 8-OHdG-positive staining in non-ischemic control animals in both WT and Immp2l$^{+/-}$ mice (Fig. 4, left column). The total number of 8-OHdG-positive cells increased in both cortical and striatal structures at 5-h of recovery with no significant difference between Immp2l$^{+/-}$ and WT animals (Fig. 4, middle column). The number of 8-OHdG-positive neurons further increased at 24-h of recovery in

both cortex and striatum with a more significant increase in Immp2l$^{+/-}$ than in WT animals (Fig. 4, right column).

Mitochondrial functional performance

To verify if lmmp2l deficiency affectes mitochondrial functional performance, we measured oxygen consumption at state 3 and state 4 in order to determine respiratory control ratio (state 3/4) and then measured FCCP induced maximum increase in oxygen consumption for mitochondrial respiratory capacity (MRC) using NADH-(glutamate and malate) and $FADH_2$-linked (succinate) substrates. As summarized in Table 1, RCR, which reflects the coupling of respiration to phosphorylation, is ~15 and 10 % higher on complex I and II dependant substrates, respectively, in Immp2l$^{+/-}$ as compared to WT control mice at baseline. In contrast, RCR decreased significantly following ischemia/reperfusion in both sets of animals with a more profound decrease being observed in Immp2l$^{+/-}$ mice. Therefore, RCR decreased about 35 and 5 % for complex I and II, respectively, in WT mice, whereas the decreases were around 55% and 18 % (complex I and II) in Immp2l$^{+/-}$ mice when compared with their non-ischemic controls.

The MRC that reflects the FCCP-induced maximum respiration was higher (18 and 17 %) with complex I and II dependant substrate in non-ischemic Immp2l$^{+/-}$ as compared to WT animals. In contrast, cerebral ischemia significantly reduced the capacity in Immp2l$^{+/-}$ as compared to WT. Thus 26 and 30% of reduction in MRC was observed in Immp2l$^{+/-}$ mice as compared to 0 and 20% decrease in WT animals (Table 1).

Mitochondrial respiratory chain complex activities

Measurement of mitochondrial complex I, II+III, and IV activities using specific substrate-inhibitors (Fig 5A and 5B) revealed that the activity of each complex was slightly higher in Immp2l$^{+/-}$ animals than in WT mice without being subjected to ischemia ($p<0.05$). Transient MCAO significantly suppressed the activity of complex I in WT mice (43% of control value). The activities of complex II+III and IV were also decreased to 65% and 54% of the control levels but did not reach statistical significance. Compared to WT animals, Immp2l$^{+/-}$ mice induced a much pronounced pan-inhibition to the activities of complex I, II +III and IV. Therefore the activities were reduced to 28%, 43% and 44% of the control values for complex I, II+III and IV, respectively at 5-h of reflow in Immp2l$^{+/-}$ mice.

Discussion

Our results provide the first *in vivo* study demonstrating that Immp2l$^{+/-}$ significantly enlarges infarct volume and increases DNA oxidative damage after transient MCAO. This damage was not due to vasculature abnormalities, as no major differences in the major cerebral vasculature were found between wild-type and Immp2l +/− mice. At present stage we could not rule out the contribution of blood circulation since reduced nitric oxide availability has been reported in homozygous Immp2l mice (Lu et al., 2008). We are conducting microvascular patency studies using these mice to further clarify the contribution of blood circulation to the damage. The detrimental effects of Immp2l deficiency to ischemic brain are most likely due to loss of activity of Immp2l, resulting in increased ROS production. As shown in Fig. 3, $\bullet O_2^-$ productions were significantly increased after only 5-h reperfusion in both the cortex and striatum of Immp2l$^{+/-}$ mice compared to WT mice at an identical reperfusion stage. Consequently, enhanced DNA oxidative damage was evident in Immp2l$^{+/-}$ mice at 24-h reperfusion (Fig. 3). Increased $\bullet O_2^-$ production in brain, sperm and testis has been observed in unchallenged homozygous Immp2l$^{-/-}$ mice that exhibited hyperpolarization of mitochondrial inner membrane potential and incomplete processing of Cyc1 (Lu et al., 2008). In addition, the higher production of ROS in Immp2l deleted mice

may be associated with increased vulnerability to brain damage following cerebral ischemia since Immp2l mutation increase the early onset of aging process (George et al., 2011) and age is an important attributor of stroke. Immp2l uses GPD2 and Cyc1 as substrates (Esser et al., 2004; Lu et al., 2008). The cytosolic GPD2 transports electrons from cytosolic NADH to mitochondria via malate-aspartate shuttle. The mitochondrial GPD2 oxidizes FAD+ to $FADH_2$. Therefore, GPD2 plays an important role in energy metabolism and oxidation in the mitochondria (Alfadda et al., 2004). Previous studies in Drosophila mitochondria have shown that GPD produces $\bullet O_2^-$ (Miwa and Brand, 2004). In the study published by Lu and colleagues, GPD2 was incompletely processed in both homo- and hetero-zygous Immp2l mutant mice (Figure 2C, Lu et al 2008). Incomplete process of GPD2 may lead to metabolic and mitochondrial abnormalities that need to be further characterized.

Cyc1 is a major component in mitochondrial complex III. Cyc1 is processed in a two-step reaction, where the second processing step required for the maturation of Cyc1 is mediated by Immp2l. The incomplete processing of Cyc1 could disturb mitochondrial electron transport, resulting in increased production of $\bullet O_2^-$. Increased ROS production has been reported to promote formation of a mitochondrial permeability transition pore that permits release of mitochondrial proteins and thereby activation of cell death pathways (Kroemer et al., 2007; Zhu et al. 2007; Leung and Halestrap, 2008; Ryu et al., 2010). Our parallel study using the same animal protocol has revealed that cleaved caspase-3 and AIF protein levels in the nuclear fractions of the Immp2l+/− mice increased significantly at 5-h of reperfusion (Ma et al unpublished date). These data suggest Immp2l plays an important role in maintaining normal mitochondrial function and in mediating cell death after ischemic stroke.

Our results demonstrated that $Immp2l^{+/-}$ impaired mitochondrial functional performance after transient MCAO. Mitochondria are vital for both cell survival and death. Dysfunctional mitochondria limit energy production by inhibition of ADP phosphorylation and causing ATP depletion. In addition, failure to restore the normal mitochondrial function during reperfusion after ischemia is associated with energy collapse and further deterioration of mitochondrial function (Rehncrona et al., 1979). We observed that RCR decreased more markedly at 5-h of reperfusion following 1-h MCAO in $Immp2l^{+/-}$ mice, suggesting that $Immp2l^{+/-}$ mice were more vulnerable to ischemia and reperfusion injury, probably due to defects at the ETC level (Rehncrona et al., 1979). The exacerbated mitochondrial dysfunction observed in $Immp2l^{+/-}$ mice probably accounts for the enlargement of infarct volume. In addition, the present study revealed the increased impairment of mitochondrial respiratory capacity in $Immp2l^{+/-}$ mice while mitochondrial respiratory capacity remained only partially affected (complex II substrate) or unaffected (complex I substrate) in WT mice. Since the maximal rate of uncoupled respiration was used to measure MCR, our results also suggest that $Immp2l^{+/-}$ affected mitochondrial capacity more prominently after stroke as compared to WT animals.

Our results showed that the enzymatic activities of mitochondrial respiratory complexes were slightly higher in $Immp2l^{+/-}$ than in WT mice. This is consistent with the reported evidence of higher complex I activity in homozygous mutant (Lu et al 2008). It is not clear whether the increased activity observed in the present study is a phenotype of $Immp2l^{+/-}$ mice at cellular level, or hyperactive mitochondria due to incomplete processing of Immp2l substrate GPD2. It has been reported that deletion of GPD2 gene in mouse leads to high ratio of NADH to NAD (Alfadda et al., 2004). This could be a potential explanation for our observation. Among the detected complexes, only complex I activity was reduced after ischemia in WT mice. In contrast, the activities of all detected mitochondrial complexes (I, II+III and IV) were significantly suppressed in the $Immp2l^{+/-}$ mice, implying that dysfunction of Immp2l caused additional inhibition to the mitochondrial complexes. The

mitochondrial complexes are very sensitive to oxidative stress and partially inhibited complex I leads to enhanced ROS production (Robinson, 1998; Kudin et al., 2004). Since both complex I and complex III are important sources of ROS production, particularly in the brain mitochondria (Kushnareva et al., 2002), it is reasonable to hypothesize that pan-suppression of mitochondrial complexes in Immp2l$^{+/-}$ mice may be related to greater production of ROS, and thereby increased brain damage following cerebral ischemia.

In summary, heterozygous Immp2l mutation enlarged infarct volume at 24-h of recovery following a transient MCAO of 1-h duration compared to WT animals. This is probably due to increased $\bullet O_2^-$ production and corresponding DNA oxidative damage. Mitochondrial experiments indicate that mitochondrial respiratory function and complex activities were impaired in early reperfusion phase of the Immp2l$^{+/-}$ mice. Deficiency in Immp2l increases the susceptibility of brain cells to ischemia and reperfusion injury. These data suggest that mitochondrial Immp2l plays an important role in cells' ability to cope with and recover from stress.

Acknowledgments

This work is supported by a grant from National Institute of Health (7R01 DK075476). The Biomanufacturing Research Institute and Technology Enterprise (BRITE) is partially funded by the Golden Leaf Foundation.

Abbreviations

CCA	common carotid artery
Cyc1	cytochrome c1
DHE	dihydroethidine
ETC	electron transport chain
GPD2	glycerol phosphate dehydrogenase 2
GPXs	glutathione peroxidases
Imp	mitochoncdrial inner membrane peptidase
Immp2l	Imp1 inner mitochondrial membrane peptidase- like
Immp2l$^{-/-}$	homozygous Immp2l mutant
Immp2l$^{+/-}$	heterozygous Immp2l mutant
MCAO	middle cerebral artery occlusion
MRC	mitochondrial respiratory capacity
mPTP	mitochondrial permeability transition pore
8-OHdG	8-hydroxy-2-deoxyguanosine
RCR	respiratory control ratio
ROS	reactive oxygen species
SOD	superoxide dismutase
TTC	2,3,5-triphenyltetrazolium chloride
WT	wild-type

References

Alfadda A, DosSantos RA, Stepanyan Z, Marrif H, Silva JE. Mice with deletion of the mitochondrial glycerol-3-phosphate dehydrogenase gene exhibit a thrifty phenotype: effect of gender. Am J Physiol Regul Integr Comp Physiol. 2004; 287:R147–156. [PubMed: 15031134]

Behrens M, Michaelis G, Pratje E. Mitochondrial inner membrane protease 1 of Saccharomyces cerevisiae shows sequence similarity to the Escherichia coli leader peptidase. Mol Gen Genet. 1991; 228:167–176. [PubMed: 1886606]

Chen J, Nagayama T, Jin K, Stetler RA, Zhu RL, Graham SH, Simon RP. Induction of caspase-3-like protease may mediate delayed neuronal death in the hippocampus after transient cerebral ischemia. J Neurosci. 1998; 18:4914–4928. [PubMed: 9634557]

Crompton M, Barksby E, Johnson N, Capano M. Mitochondrial intermembrane junctional complexes and their involvement in cell death. Biochimie. 2002; 84:143–152. [PubMed: 12022945]

Di Lisa F, Canton M, Menabo R, Dodoni G, Bernardi P. Mitochondria and reperfusion injury. The role of permeability transition. Basic Res Cardiol. 2003; 98:235–241. [PubMed: 12835952]

Esser K, Jan PS, Pratje E, Michaelis G. The mitochondrial IMP peptidase of yeast: functional analysis of domains and identification of Gut2 as a new natural substrate. Mol Genet Genomics. 2004; 271:616–626. [PubMed: 15118906]

George SK, Jiao Y, Bishop CE, Lu B. Mitochondrial peptidase IMMP2L mutation causes early onset of age-associated disorders and impairs adult stem cell self renewal. Aging Cell. 2011 [Epub ahead of print]. 10.1111/j.1474-9726.2011.00686.x

Haines BA, Mehta SL, Pratt SM, Warden CH, Li PA. Deletion of mitochondrial uncoupling protein-2 increases ischemic brain damage after transient focal ischemia by altering gene expression patterns and enhancing inflammatory cytokines. J Cereb Blood Flow Metab. 2010; 30:1825–1833. [PubMed: 20407461]

Halestrap AP. Calcium, mitochondria and reperfusion injury: a pore way to die. Biochem Soc Trans. 2006; 34:232–237. [PubMed: 16545083]

Kroemer G, Galluzzi L, Brenner C. Mitochondrial membrane permeabilization in cell death. Physiol Rev. 2007; 87:99–163. [PubMed: 17237344]

Kudin AP, Kudina TA, Seyfried J, Vielhaber S, Beck H, Elger CE, Kunz WS. Seizure-dependent modulation of mitochondrial oxidative phosphorylation in rat hippocampus. Eur J Neurosci. 2004; 15:1105–1114. [PubMed: 11982622]

Kuizumi J, Yoshida Y, Nakazawa T, Ooneda G. Experimental studies of ischemic brain edema. 1 A new experimental model of cerebral embolism in rats in which recirculation can be introduced in the ischemic area. Jpn J Stroke. 1986; 8:1–8.

Kushnareva Y, Murphy AN, Andreyev A. Complex I-mediated reactive oxygen species generation: modulation by cytochrome c and NAD(P)+ oxidation-reduction state. Biochem J. 2002; 368:545–553. [PubMed: 12180906]

Leung AW, Halestrap AP. Recent progress in elucidating the molecular mechanism of the mitochondrial permeability transition pore. Biochim Biophys Acta. 2008; 1777:946–952. [PubMed: 18407825]

Lu B, Poirier C, Gaspar T, Gratzke C, Harrison W, Busija D, Matzuk MM, Andersson KE, Overbeek PA, Bishop CE. A mutation in the inner mitochondrial membrane peptidase 2-like gene (Immp2l) affects mitochondrial function and impairs fertility in mice. Biol Reprod. 2008; 78:601–610. [PubMed: 18094351]

Miwa S, Brand MD. The topology of superoxide production by complex III and glycerol 3-phosphate dehydrogenase in Drosophila mitochondria. Biochim Biophys Acta. 2005; 1709:214–219. [PubMed: 16140258]

Martin L. Mitochondrial and cell death mechanisms in neurodegenerative diseases. Pharmaceuticals. 2010; 3:839–915. [PubMed: 21258649]

Nunnari J, Fox TD, Walter P. A mitochondrial protease with two catalytic subunits of nonoverlapping specificities. Science. 1993; 262:1997–2004. [PubMed: 8266095]

Petek E, Windpassinger C, Vincent JB, Cheung J, Boright AP, Scherer SW, Kroisel PM, Wagner K. Disruption of a novel gene (IMMP2L) by a breakpoint in 7q31 associated with Tourette syndrome. Am J Hum Genet. 2001; 68:848–858. [PubMed: 11254443]

Rehncrona S, Smith ML, Siesjö BK. Recovery of brain mitochondrial function in the rat after complete and incomplete cerebral ischemia. Stroke. 1979; 10:437–446. [PubMed: 505482]

Robinson BH. Human complex I deficiency: clinical spectrum and involvement of oxygen free radicals in the pathogenicity of the defect. Biochim Biophys Acta. 1998; 1364:271–286. [PubMed: 9593934]

Ryu SY, Peixoto PM, Teijido O, Dejean LM, Kinnally KW. Role of mitochondrial ion channels in cell death. Biofactors. 2010; 36:255–263. [PubMed: 20623547]

Soler R, Fullhase C, Lu B, Bishop CE, Andersson KE. Bladder dysfunction in a new mutant mouse model with increased superoxide-lack of nitric oxide? J Urol. 2010; 183:780–785. [PubMed: 20022053]

Yu SW, Wang Y, Frydenlund DS, Ottersen OP, Dawson VL, Dawson TM. Outer mitochondrial membrane localization of apoptosis-inducing factor: mechanistic implications for release. ASN Neuro. 2009:1.10.1042/AN20090046

Zhao H, Kalivendi S, Zhang H, Joseph J, Nithipatikom K, Vasquez-Vivar J, Kalyanaraman B. Superoxide reacts with hydroethidine but forms a fluorescent product that is distinctly different from ethidium: potential implications in intracellular fluorescence detection of superoxide. Free Radic Biol Med. 2003; 34:1359–1368. [PubMed: 12757846]

Zhu C, Wang X, Huang Z, Qiu L, Xu F, Vahsen N, Nilsson M, Eriksson PS, Hagberg H, Culmsee C, Plesnila N, Kroemer G, Blomgren K. Apoptosis-inducing factor is a major contributor to neuronal loss induced by neonatal cerebral hypoxia-ischemia. Cell Death Differ. 2007; 14:775–784. [PubMed: 17039248]

Highlights

- Immp2l deficiency increases infarct volume after focal cerebral ischemic stroke.
- cerebral vasculature is normal in Immp2l deficient mice.
- Enlarged infarct volume in Immp2l deficient mice is associated with enhanced production of superoxide.
- Defect in Immp2l suppresses mitochondrial respiration and respiratory complex activities after stroke.

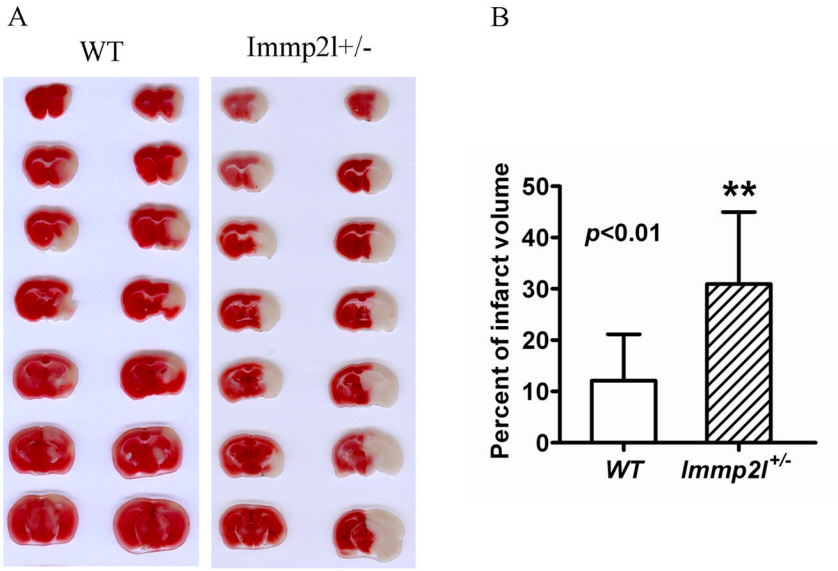

Fig. 1.

Brain infarct volume. ***A,*** Representative TTC stained brain sections showing infarct volume (white color) at 24-h of reperfusion following 1-h of MCAO in WT and Immp2l$^{+/-}$ mice. ***B,*** Bar graph summarizes the mean values of cerebral infarction in WT (n=10) and Immp2l$^{+/-}$ mice (n=7). Infarct volume enlarged significantly in Immp2l$^{+/-}$ mice. **p<0.01.

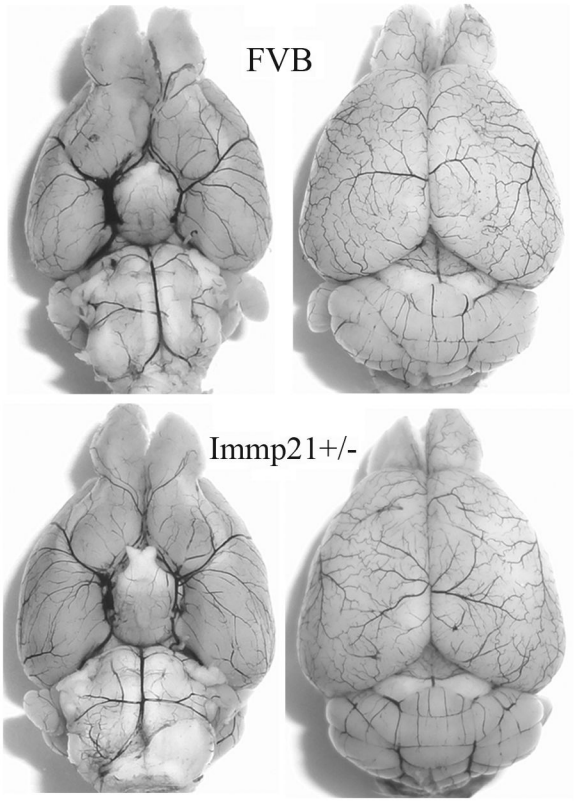

Fig. 2.

Cerebral vasculature. Mice (n=3 each group) were perfused with Indian black ink to determine whether there were vascular abnormalities in the Immp2$^{+/-}$ mice. The Circle of Willis, anterior cerebral arteries, middle cerebral arteries, and posterior arteries all appear normal as compared with those in WT (FVB) controls.

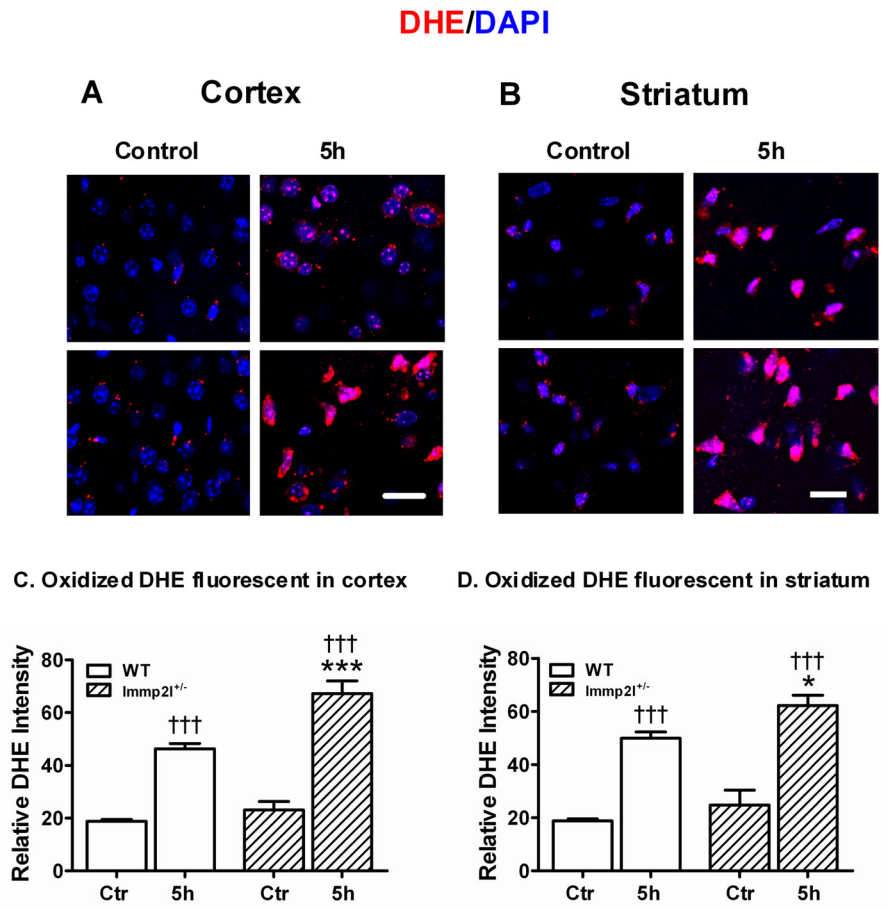

Fig. 3.

Superoxide production detected by DHE. Panels **A and B** are representative photomicrograms showing $\bullet O_2^-$ production in WT and Immp2l$^{+/-}$ mice. Animals were injected with DHE 30-min prior to being subjected to control or 1-h MCAO with 5-h reperfusion. Sections were collected from the cortex (**A**) and striatum (**B**). Nuclei were labeled with DAPI. Magnification, 400X. Scale bar = 50 μm. Panels **C and D** are summarized DHE fluorescent intensity in the cortex (C) and striatum (D). Data are presented as means ± s.d. (n = 4 per time point). $^{\dagger\dagger\dagger}P < 0.001$ *vs*. sham-operated control in same type of animals, and $^{*}P < 0.05$, $^{***}P < 0.001$ *vs*. WT at an identical time point.

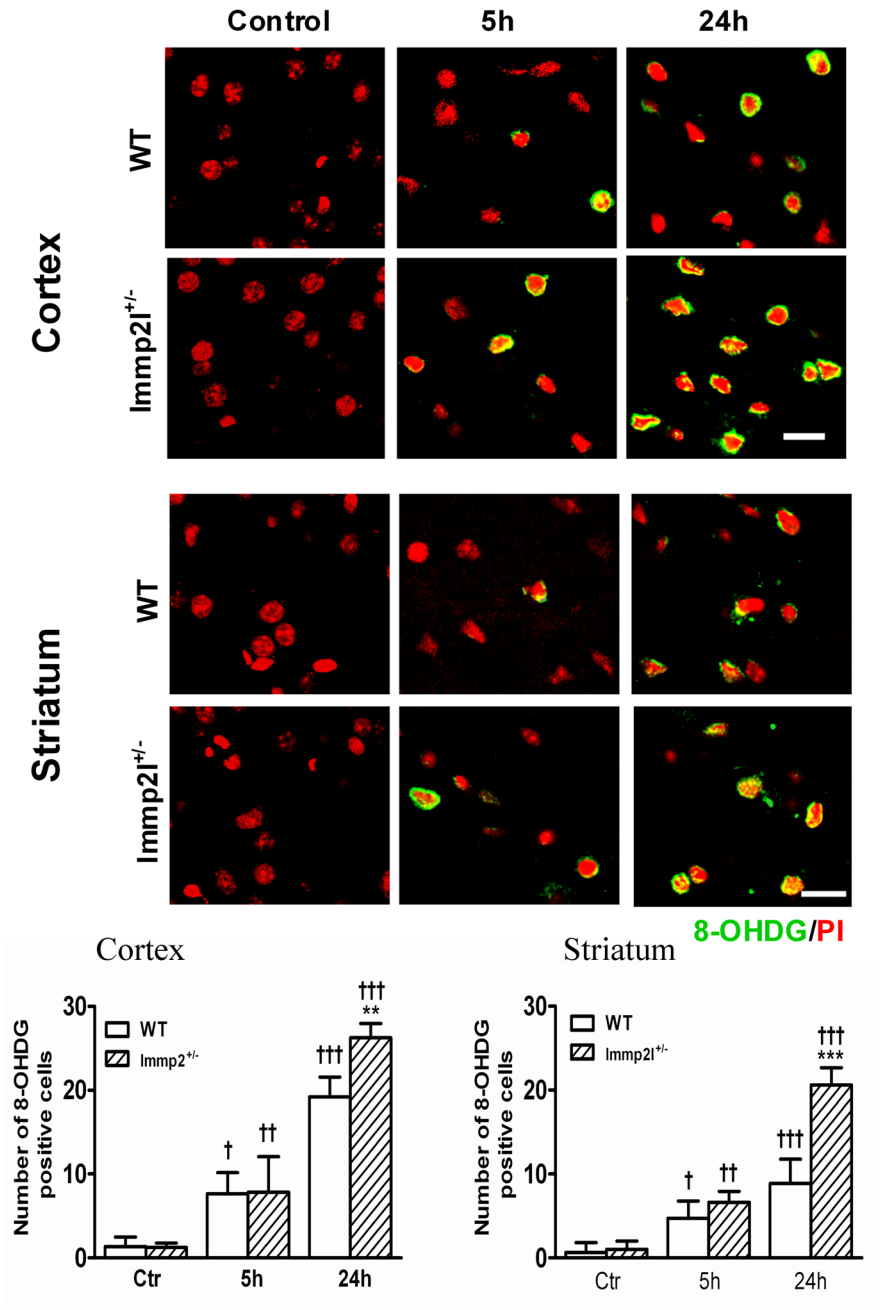

Fig. 4.

DNA oxidative damage detected by 8-OHdG immunohistochemistry. Fluorescent stainned brain sections show DNA oxidative damage in the cortex and striatum of the WT and Immp2l$^{+/-}$ mice. Animals were subjected to sham-operation (Control), or 1-h MCAO with 5- or 24-h of reperfusion (n=4 each group). Nuclei were labeled with propidium iodide (PI). Magnification, 400X. Scale bar = 50 μm. Bar graphs show the number of 8-OHdG positive cells per section in the cortex and striatum. Data are presented as means ± s.d. $^{\dagger}P < 0.05$, $^{\dagger\dagger}P < 0.01$, $^{\dagger\dagger\dagger}P < 0.001$ *vs*. sham-operated control in same type of animals, and $^{**}P < 0.01$, $^{***}P < 0.001$ *vs*. WT at an identical time point.

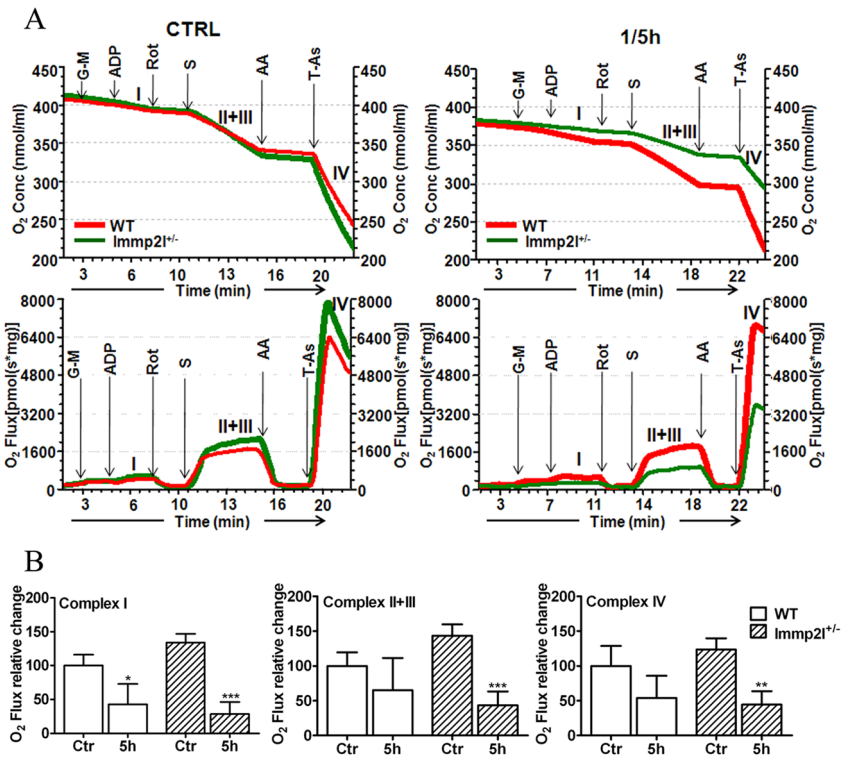

Fig. 5.

Mitochondrial respiratory rate at different complexes. **A**, Upper panel shows Oxygen consumption in control and 1-h MCAO plus 5-h reperfusion (1/5h) in FVB and Immp2l$^{+/-}$ mice brain mitochondria (n=3 each group). Lower panel shows the respiratory rate following addition of substrates. The respiration rate, hence oxygen utilization, was initiated by the addition of glutamate and malate (G-M) for complex I, succinate (S) and rotenone (rot) for complex II+III, and TMPD/ascorbate (T-As) and antimycin A (AA) for complex IV. The activity of each complex was calculated from the difference in reduction in oxygen content in the presence of specific substrate and specific inhibitor. **B**, Summarized data show activity of each complex in control (Ctr) and ischemia plus 5-h reperfusion (5h). Data are presented as means ± s.d. (n = 4 per time point). *P<0.05, **p<0.001 and ***p<0.001.

Table 1

Respiratory control ratio (RCR) Mitochondrial respiratory capacity (MRC) and OXPHOS control ratio (OCR) of brain mitochondria using glutamate +malate (Glu+Mal) or succinate (Succ) as substrates

	Substrate	FVB		Immp2l$^{+/-}$	
		Ctr	5 h	Ctr	5h
RCR	Glu+Mal	5.04±0.66	3.37±0.16**	5.97±0.40	3.19±0.11***
	Succ	3.18±0.07	3.0±0.01	3.48±0.08	2.86±0.07**
MRC	Glu+Mal	1.0±0.05	0.99±0.04	1.18±0.12	0.87±0.02*
	Succ	1.0±0.02	0.79±0.09*	1.17±0.01	0.82±0.10**
OCR	Glu+Mal	0.61±0.03	0.45±0.03**	0.76±0.07	0.51±0.03***
	Succinate	1.0±0.01	0.91±0.01**	1.0±0.02	0.80±0.01***